22nd International Conference on
Harmonisation within Atmospheric Dispersion Modelling for Regulatory Purposes
10-14 June 2024, Pärnu, Estonia

# ENHANCED DEEP LEARNING ARCHITECTURE FOR 3D AIR POLLUTION DISPERSION FORECASTING

*Mouhcine Mendil[1], Paul Novello[1], Sylvain Leirens[2], Christophe Duchenne[3] and Patrick Armand[3]*

[1] IRT Saint Exupéry, Toulouse, France
[2] Univ. Grenoble Alpes, CEA, Leti, F-38000 Grenoble
[3] CEA, DAM, DIF, F-91297 Arpajon, France

**Abstract**: Urban air pollution is a major concern that significantly impacts the environment and public health. In this context, machine learning has enabled the development of surrogate models, which have proven to be valuable tools for simulating atmospheric pollution. Our previous work introduced the MCxM, a new approach to learning air pollution dispersion in urban environments. This framework allows for the prediction of 2D concentration fields by applying a series of masking and correction operations that gradually incorporate the influence of obstacles into the physics of pollutant transport and dispersion. In this paper, we propose to enhance the MCxM architecture by extending its capabilities to predict three-dimensional concentration fields. These enhancements mainly involve the integration of architectural blocks to scale and approximate the underlying physics. To validate the effectiveness of our approach, we used synthetic integrated concentration data generated by the PMSS modeling system, considering extensive twin experiments in the French cities of Grenoble and Paris. The results indicate that the accuracy of the predicted integrated concentration field has improved significantly compared to our previous work.

***Keywords:*** *Surrogate model, deep learning, synthetic data, urban pollution, dispersion modelling, simulation.*

## INTRODUCTION

The accurate forecasting of urban air pollution is crucial for public health advisories, environmental protection, and urban planning. Traditionally, this has been approached through high-fidelity CFD models, which simulate the physics of atmospheric flows and chemical processes to predict the transport and dispersion of pollutants. However, these models often require extensive computational resources.
Surrogate modeling is a crucial technique that provides efficient alternatives to computationally expensive simulations, offering significant reductions in computational time and resources while maintaining acceptable accuracy. The development of surrogate models in the context of physics encompasses several advanced methodologies, primarily leveraging machine learning technologies. Physics-Informed Neural Networks (PINNs) (Cai et al., 2021) incorporate physical laws into the learning process, usually by adding a residual of PDEs in the loss function, which helps in training data-efficient models that adhere closely to the underlying physical principles to approximate the PDE solution. When there is an abundance of data (experimental or synthetic), data-driven deep learning models are favored as surrogate models because they can model complex spatial and temporal nonlinear dynamics. Several DNN architectures have been employed to model airflow in different use cases. Usually, these studies learn to infer the solution in a fixed PDE instance, which generally entails retraining the model when the setting changes (for example, the building topology) (Calzolari et al., 2021). A relatively novel class of methods employs neural networks to learn operators (a mapping between function spaces), which are conceptually generalizable and can solve different families of PDEs without the need for retraining. For example, DeepONets (Lu et al., 2021) and

FNOs (Li et al., 2020) enable the learning of a generalizable operator that can solve different instances (initial and boundary conditions) of the underlying PDE.

Our previous work introduced the MCxM, an innovative approach designed to address urban pollution dispersion challenges. The MCxM framework improved upon traditional methods by incorporating domain-specific knowledge through a series of masking and correction operations, enhancing the model's ability to account for the effects of urban obstacles on pollutant dispersion. This paper proposes enhancements to the MCxM architecture to extend its capabilities into three-dimensional (3D) space. This advancement is crucial as it allows for a more accurate representation of pollution dispersion, which is inherently a 3D process. The enhanced model includes a series of complementary preprocessing steps and new architectural blocks to scale the model to approximate complex physics involved in pollutant transport and dispersion in three dimensions.

## MODEL DESCRIPTION

In our previous study (Mendil et al., 2022), we developed a deep learning-based approach called MCxM to predict the concentration of pollutants accidentally released in urban areas. Such an approach is extended to 3D by scaling the masking and correction operations. Instead of 2D inputs, we provide the MCxM-3D with a couple of 3D tensors: a 3D building mask indicating the presence or absence of buildings in different locations and heights and a prior integrated concentration field derived from the 3D Gaussian plume in a flat terrain under specified stability conditions.

An instance of the MCxM model takes as inputs a binary map in $\mathbb{R}^{m\times m\times h}$ representing the urban area and a prior Gaussian plume in $\mathbb{R}^{m\times m\times h}$ derived for neutral stability conditions and stationary wind properties (direction and speed), where $m$ is the number of cells in each direction of the horizontal plane and $h$ is the number of levels along the $z$-axis. The Gaussian plume model is a well-established approximation of pollutant dispersion in a flat environment without any obstacles. However, MCxM aims to refine this model by considering the physical interactions between airflow and buildings, such as trajectory changes and mechanical turbulence. To achieve this, MCxM employs two primary operations: masking and correction. Masking is a point-wise multiplication between the binary building map and a concentration field, effectively enforcing spatial constraints associated with the urban area. Correction involves a deep learning model trained to approximate pollutant transport and dispersion physics. Figure 1 illustrates the architecture of the extended MCxM.

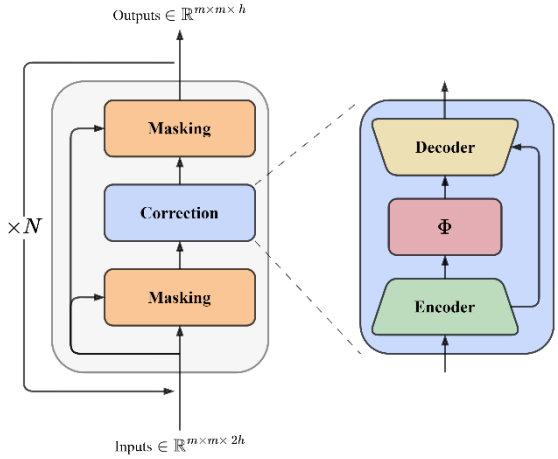


**Figure 1**: MCxM extended architecture.

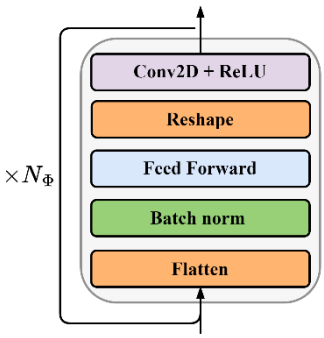


**Figure 2**: Non-linear operator (Φ) in the correction block.

The sequence of masking and correction can be structured as a recurrent neural network and reiterated $N$ times to progressively model the impact of different obstacles on the expanding polluted areas.

The correction block can be implemented using various models. In our previous study (Mendil et al., 2022), the correction block operated on inputs of dimension $m \times m$ ($h = 1$) and consisted of a series of feed-forward, ReLU activation, and batch normalization layers. We propose a new instance of the correction block that combines the strengths of convolutional neural networks with the capabilities of neural operators. The encoder/decoder consists of a Unet-like architecture (Ronneberger et al., 2015), and Φ is represented by a non-linear neural operator in the latent space. More precisely:

- The encoder, represented in Figure 3, extracts features from the input 3D concentration field in $\mathbb{R}^{m \times m \times h}$ and building topography in $\mathbb{R}^{m \times m \times h}$. It comprises $N_e$ contracting blocks, each consisting of two convolutional layers followed by ReLU activation, a batch normalization layer, and a max pooling layer.
- The non-linear operator Φ, represented in Figure 2, processes the encoder's latent state through a series of batch normalization, linear feed-forward, and convolution layers. According to (Kovachki et al., 2023), using a composition of convolution and nonlinear activations enables the approximation of PDE solution operators, with the goal of deriving the general physical processes that govern pollutant transport and dispersion.
- The decoder, shown in Figure 4, builds the final 3D concentration field based on the transformed latent representation. It is composed of $N_e$ expanding blocks, each featuring a transpose convolutional layer, two convolutional layers followed by ReLU activation, and a batch normalization layer. As for Unet, note the residual connection on the feature maps the encoding block provides. Finally, a 1x1 convolution outputs the final integrated concentration field in $\mathbb{R}^{m \times m \times h}$.

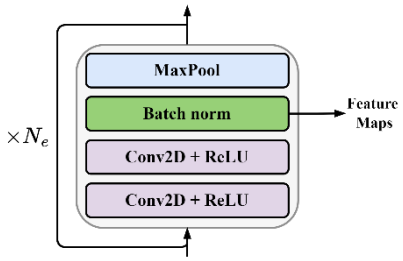


**Figure 3**: Encoder component in the correction block. The skip connections take multiscaled feature maps to the decoder block.

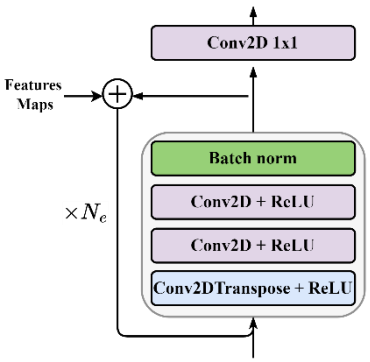


**Figure 4**: Decoder component in the correction block. The multiscale feature maps come from the encoder block.

## EXPERIMENT SETTINGS

Our approach was tested in two French cities, Grenoble and Paris, which have a typical European architectural style. The buildings date back to the 19th and 20th centuries and are predominantly 20 to 25 meters tall. The training dataset is composed of several instances of 3D integrated concentration over 2 hours, generated by Parallel-Micro-SWIFT-SPRAY (PMSS) (Oldrini et al., 2017), a multi-scale 3D numerical modeling system of atmospheric transport and dispersion. The computational domain within PMSS encompasses an urban neighborhood of the French city of Grenoble. This domain is defined by a high-resolution grid, maintaining both horizontal and vertical resolutions of 2 meters up to the building heights. Beyond this point, as the simulation extends vertically above the building tops, the vertical resolution progressively coarsens while the horizontal resolution remains constant.

The emission source is considered in different hypothetical locations given 108 stationary weather conditions above the urban canopy, built from a combination of 36 values of wind direction $\theta$ [°] ∈ {0, 10,20, …,350} and three values of wind speed $v$ [$m.\ s-1$ ] ∈ {1.5, 3.5, 6}. The test dataset is constructed similarly in the Opera district of Paris. A point source produces an instantaneous fictitious emission of a

unit mass of the pollutant (gas or particle matter) at a fixed height $h_S = 2$ m for all experiments. For a given initialization (source location and wind conditions), PMSS simulates the steady 3D wind field and the unsteady 3D concentration fields for two hours.
The data preparation consists of several steps to optimize the learning model. First, we integrate the concentration over the entire simulation period of two hours, thereby eliminating the temporal dimension from the analysis. Then, the 3D concentration fields and the corresponding buildings tensors are centered on the origin of emissions to ensure that the model learns dispersion patterns relative to the source, irrespective of its absolute location in the input data. Following this, we spatially subsample the data to achieve tensors of shape $m \times m \times h$, which simplifies the training process. Finally, we implement data augmentation that includes flipping the fields along the vertical axis to enhance the robustness and prevent overfitting.

**Table 1.** Hyperparameters of the extended MCxM

| **m** | **h** | $N$ | $N_e$ | $N_\Phi$ | **Encoder/decoder Conv2D Kernels** | $\Phi$ **Conv2D Kernels** | $\Phi$ **Feed-forward # of Neurons** | $\Phi$ **Conv2D 1x1 Kernel** |
|---|---|---|---|---|---|---|---|---|
| 100 | 6 | 1 | 2 | 2 | $3 \times 3 \times 32$<br>$3 \times 3 \times 64$ | $3 \times 3 \times 64$ | 32 | $1 \times 1 \times 6$ |

Throughout the training, regularization strategies were used to make learning tractable and improve the generalization error, mainly exponential decay of the learning rate and early stopping. Mean Squared Logarithmic Error (MSLE) is used as a loss function, with RMSProp serving as the optimizer. Other hyperparameters are summarized in the Table 1.

## RESULTS

In our previous work, the MCxM achieved a MSLE of 0.96 on the Paris test set. Figure 5 shows the MSLE achieved by the extended MCxM across different vertical slices. Notably, the model exhibits higher accuracy at lower altitudes, closely approximating the 3D integrated concentration field. At the height of the emission source, the MSLE is approximately 0.33, indicating a clear improvement over the previous MCxM that primarily learned from horizontal slices of 3D concentration fields. The results show that the consideration of 3D concentration fields during training, as well as relying on dimension reduction and neural operator architectures have significantly improved our model's performance. However, the accuracy diminishes at higher altitudes, with an MSLE of around 0.5. This issue will be further investigated in future work.

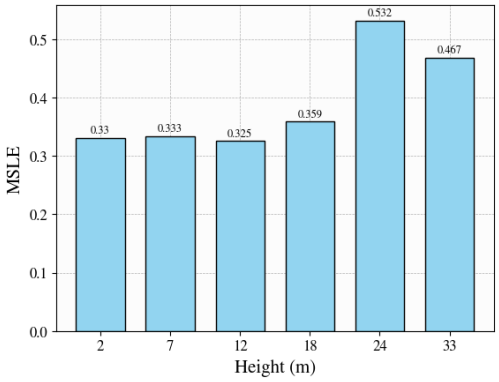


**Figure 5**: MSLE achieved at different heights by the extended MCxM on the test dataset in Paris.

Figure 6 presents an instance of predicted and simulated concentration fields at various heights. The shadowed areas in the visualization highlight the presence of buildings. Overall, the results align with the simulations (ground-truth). Notably, at lower heights, the closed 2D contours located south of the emission source would typically be inaccessible to pollutants if not considering the comprehensive 3D airflow. This outcome suggests that the model effectively captures some 3D interactions between building structures and airflow, as well as the influence of street intersections on the trajectory of pollutants.

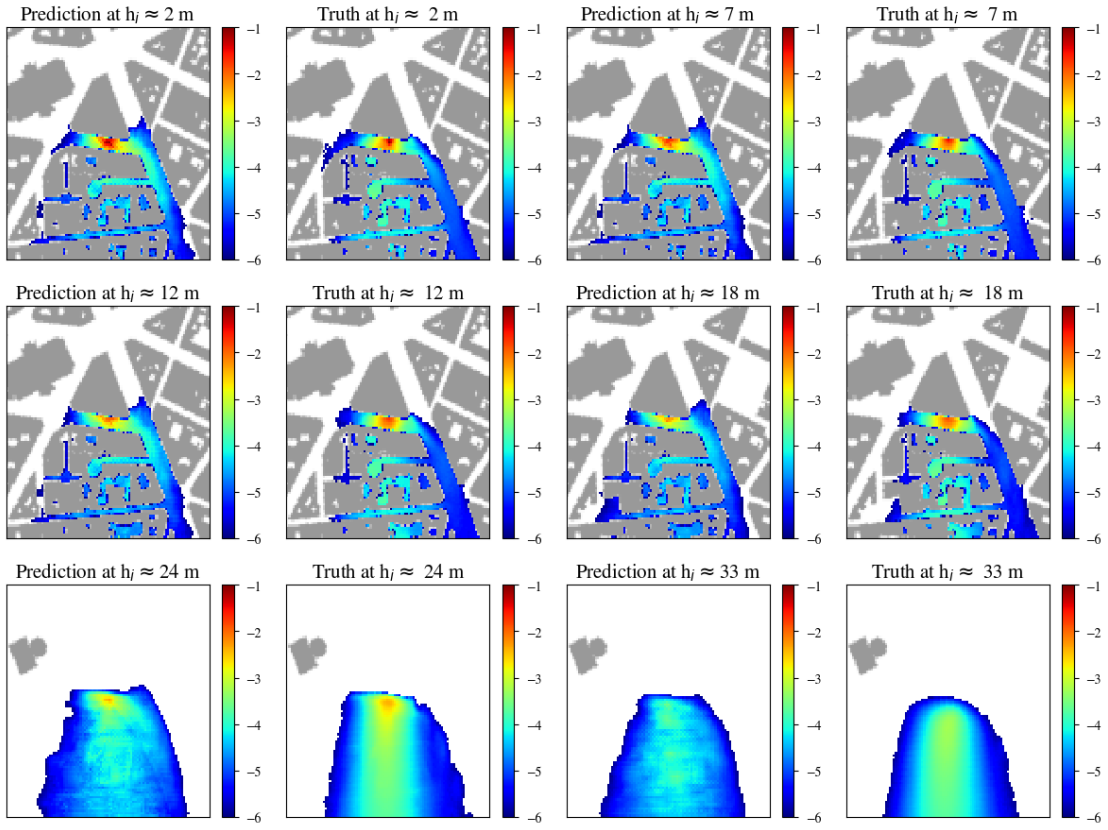


**Figure 6**: Examples of predicted and ground-truth (synthetic) integrated concentration field [unit. s m−3/unit. released] in Paris (logarithmic scale) at different heights $h_i$.

## CONCLUSION

By extending learning to 3D air pollution dispersion, we enable the model to integrate more comprehensive spatial data, including vertical variations that are critical in urban settings where buildings significantly influence airflow. The improved MCxM approach relies on scaled masking and correction operations that combine the strengths of physics priors, convolutional neural networks, and neural operators. The extended MCxM has demonstrated significantly lower MSLE and, thus, better predictive performance, particularly at lower altitudes where the concentration of pollutants is often the highest and most critical for urban populations.

## REFERENCES

Cai, S., Z. Mao, Z. Wang, M. Yin, and G. E. Karniadakis, 2021: Physics-informed neural networks (PINNs) for fluid mechanics: A review. Acta Mech. Sin., 37, 1727–1738.

Calzolari, G. and W. Liu, 2021: Deep learning to replace, improve, or aid CFD analysis in built environment applications: A review. Build. Environ., 206, 108315.

Kovachki, N., Z. Li, B. Liu, K. Azizzadenesheli, K. Bhattacharya, A. Stuart, and A. Anandkumar, 2023: Neural operator: Learning maps between function spaces with applications to PDEs. J. Mach. Learn. Res., 24, 1–97.

Li, Z., N. Kovachki, K. Azizzadenesheli, B. Liu, K. Bhattacharya, A. Stuart, and A. Anandkumar, 2020: Fourier neural operator for parametric partial differential equations. arXiv preprint arXiv:2010.08895.

Lu, L., P. Jin, G. Pang, Z. Zhang, and G. E. Karniadakis, 2021: Learning nonlinear operators via DeepONet based on the universal approximation theorem of operators. Nat. Mach. Intell., 3, 218–229.

Mendil, M., S. Leirens, P. Armand, and C. Duchenne, 2022: Hazardous atmospheric dispersion in urban areas: A Deep Learning approach for emergency pollution forecast. Environ. Model. Softw., 152, 105387.

Oldrini, O., Armand, P., Duchenne, C., Olry, C., Moussafir, J., & Tinarelli, G. (2017). Description and preliminary validation of the PMSS fast response parallel atmospheric flow and dispersion solver in complex built-up areas. Environmental Fluid Mechanics, 17, 997-1014.

Ronneberger, O., P. Fischer, and T. Brox, 2015: U-net: Convolutional networks for biomedical image segmentation. In Medical Image Computing and Computer-Assisted Intervention–MICCAI 2015: 18th International Conference, Munich, Germany, October 5-9, 2015, Proceedings, Part III, Springer Int. Publ., 18, 234–241.